Current Research in Pharmacology and Drug Discovery 8 (2025) 100216

Contents lists available at ScienceDirect

Current Research in Pharmacology and Drug Discovery

journal homepage: www.journals.elsevier.com/current-research-in-pharmacology-and-drug-discovery

ABCC1 and ABCC10 as predictive biomarkers of docetaxel treatment response in prostate cancer

Nandi Ngesi [a], Beynon Abrahams [b], Aubrey Shoko [c], Mamello Sekhoacha [a,*]

[a] Department of Pharmacology, University of the Free State, P.O. Box 339, 9300, Bloemfontein, Republic of South Africa
[b] Department of Basic Medical Sciences, University of the Free State, Bloemfontein, Republic of South Africa
[c] Centre for Proteomic and Genomics Research, 108 Albert Rd, Woodstock, Cape Town, 7925, South Africa

ARTICLE INFO

Keywords:
PCa
Chemoresistance
Docetaxel
ABC-Transporters
FFPE
Quantitative RT-PCR
Biomarker

ABSTRACT

Prostate cancer (PCa) is a leading global health burden, with a particularly high prevalence in South Africa. Despite therapeutic advancements, chemoresistance remains a major challenge, limiting the efficacy of docetaxel and contributing to treatment failure and disease progression. Multidrug resistance (MDR), primarily mediated by ATP-binding cassette (ABC) transporters such as ABCC1 and ABCC10, has been implicated in reduced chemotherapy effectiveness. This study aimed to evaluate the association between ABCC1 and ABCC10 expression levels and docetaxel treatment response in PCa patients. A retrospective case-control study was conducted using pre-treated formalin-fixed paraffin-embedded (FFPE) tissue biopsies from PCa patients. Patients were classified into good responders (cases) and poor responders (cases) based on treatment outcomes. For each patient, tumour and adjacent normal sections were excised from FFPE samples, with normal sections serving as the control group. RNA was extracted and subjected to quantitative real-time PCR (qRT-PCR) to assess ABCC1 and ABCC10 expression levels. ABCC1 and ABCC10 were significantly upregulated in tumour sections of poor responders, whereas good responders exhibited downregulated expression in tumour sections. Importantly, normal tissue sections (controls) displayed significantly lower expression levels of both transporter genes compared to tumour sections. The overexpression of ABCC1 and ABCC10 in tumour tissues, particularly in poor responders, suggests their potential role in mediating docetaxel resistance. These findings highlight ABCC1 and ABCC10 as potential predictive biomarkers for docetaxel treatment response in PCa, warranting further investigation in prospective clinical studies.

1. Introduction

PCa remains a major global health concern, with particularly high prevalence in South Africa, where it is the most frequently diagnosed malignancy among men (Sánchez et al., 2009; Cassim et al., 2021). Early detection relies on various screening methods; however, definitive diagnosis is established through histopathological examination of biopsy specimens (Sekhoacha et al., 2022). Treatment options for PCa include active surveillance, radiation therapy, surgery, hormone therapy, chemotherapy, cryotherapy, and immunotherapy, selected based on disease stage and patient-specific factors (Begicevic and Falasca, 2017). Despite therapeutic advancements, treatment resistance poses a critical challenge, leading to disease progression, relapse, and high mortality rates (Begicevic and Falasca, 2017). In cases of metastatic castration-resistant prostate cancer (mCRPC), chemotherapy—specifically docetaxel-based regimens—remains a primary treatment modality. However, multidrug resistance (MDR), a phenomenon wherein cancer cells develop resistance to multiple chemotherapeutic agents, is a major barrier to effective treatment (Kachalaki et al., 2016). Various mechanisms contribute to MDR, including decreased drug uptake, enhanced DNA damage repair, suppression of apoptosis, alterations in drug metabolism, and most notably, increased drug efflux mediated by membrane-bound transporters (Kachalaki et al., 2016; Hasan et al., 2018). Among these mechanisms, efflux transporter genes play a pivotal role in diminishing intracellular drug accumulation, thereby reducing treatment efficacy (Choi, 2005; Sone et al., 2019). A key group of efflux transporters involved in MDR is the ATP-binding cassette (ABC) transporter superfamily, which includes 49 identified genes classified into seven subfamilies (Kachalaki et al., 2016; Domenichini et al., 2019). Among these, ABCB1 (MDR1/P-glycoprotein),

* Corresponding author.
E-mail address: SekhoachaMP@ufs.ac.za (M. Sekhoacha).

https://doi.org/10.1016/j.crphar.2025.100216
Received 16 October 2024; Received in revised form 21 February 2025; Accepted 7 March 2025
Available online 14 March 2025

ABCC1 (MRP1), and ABCG2 (BCRP) have been extensively studied for their role in chemoresistance across multiple cancer types (Begicevic and Falasca, 2017). These transporters actively expel cytotoxic drugs from cancer cells, leading to decreased therapeutic efficacy.

This study specifically investigates the role of ABCC1 and ABCC10 transporter genes in mediating docetaxel resistance in prostate cancer. These genes were selected due to their known involvement in the transport of taxane-based chemotherapeutics, including docetaxel. Docetaxel, a second-generation taxane derived from the European yew tree (*Taxus baccata*), stabilizes microtubules and induces mitotic arrest, ultimately leading to apoptosis. However, its efficacy is compromised by efflux through transporters such as ABCC1, which reduces intracellular drug accumulation (Varnai et al., 2019). ABCC1 is highly expressed in prostate cancer tissues and cell lines, including DU145 and PC-3, and its expression has been associated with advanced-stage disease (Seo et al., 2020). Similarly, ABCC10 has been implicated in resistance to taxanes, including paclitaxel, docetaxel, and cabazitaxel, further emphasizing its role in treatment failure (Sone et al., 2019; Chen et al., 2024). Given their potential role in chemoresistance, evaluating the expression levels of ABCC1 and ABCC10 in prostate cancer tissues may provide insight into their prognostic and predictive value in docetaxel treatment outcomes.

This case-control study aims to examine the association between ABCC1 and ABCC10 gene expression and docetaxel treatment response in prostate cancer patients. The primary objective is to determine whether the expression of these ABC transporter genes can serve as predictive biomarkers for docetaxel resistance. By identifying gene expression patterns associated with poor treatment response, this study contributes to the growing field of pharmacogenetics, which seeks to optimize therapy based on individual genetic profiles. The findings may support the development of personalized treatment strategies, enabling clinicians to predict treatment outcomes and adjust therapeutic regimens accordingly. This could lead to the selection of alternative therapies, adjusted dosages, or combination strategies designed to circumvent resistance mechanisms, ultimately advancing precision medicine in prostate cancer management.

2. Materials and methods

2.1. FFPE biopsy samples

This retrospective case-control study was conducted using pre-treatment formalin-fixed paraffin-embedded (FFPE) prostate cancer (PCa) tissue biopsies collected from patients treated at National Public Hospital, Bloemfontein, and archived at the National Health Laboratory Services (NHLS), Universitas Academic Hospital, Bloemfontein, between 2016 and 2022. Ethical approval was obtained from the Health Sciences Research Ethics Committee at the University of the Free State, Bloemfontein (Ethical No: UFS-HSD2022/1325/3101), as well as the Free State Department of Health. Permission to access the FFPE samples was granted by the NHLS at Universitas Academic Hospital (Ethical No: PR2343021). To ensure patient confidentiality, all specimens and clinical data were anonymized, and as a result, patient consent was waived in accordance with the National Ethics Guidelines: *Department of Health Ethics in Health Research Guidelines, Processes, Structures, and Procedures* (2015). The study was conducted in adherence to the ethical principles outlined in the Declaration of Helsinki.

The study included pre-treatment FFPE tissue biopsies from PCa patients aged 40–80 years. Patients were classified as either good or poor responders based on their clinical response to docetaxel therapy. This classification was determined retrospectively through clinical records, assessing PSA levels, symptomatic improvement, and disease progression post-treatment. A total of nine patient specimens were selected for this pilot study, generating 18 tissue sections, with both tumour and adjacent normal sections excised from each sample for analysis.

The primary independent variables were the expression levels of the ABCC1 and ABCC10 transporter genes, quantified via quantitative real-time PCR (qRT-PCR). The dependent variable was the patient's response to docetaxel, categorized as good responder or poor responder. Tissue samples were sectioned at 10 μm using a microtome and collected in nuclease-free tubes. RNA extraction was performed from both tumour and normal sections using an optimized protocol. RNA purity and concentration were assessed spectrophotometrically before proceeding to qRT-PCR. Gene expression analysis was conducted using TaqMan assays specific to ABCC1 and ABCC10, with normalization to a reference gene. Relative gene expression was determined using the $2^{-\Delta\Delta Ct}$ method. Relative expression levels were compared between tumour and normal sections within each patient, as well as between good and poor responders. To minimize selection bias, only pre-treatment FFPE biopsies were included, ensuring uniformity in sample processing. Measurement bias was reduced by conducting all qRT-PCR analyses in triplicates and employing automated software for Cq value determination. Additionally, to prevent observer bias, data analysts were blinded to the patient response classification during gene expression analysis. Clinical characteristics documented for each patient included clinical stage, Gleason score, serum PSA levels, and the number of docetaxel cycles administered (see Table 1).

2.2. RNA extraction, quantification, and purity assessment

RNA was extracted from 18 tissue sections using the Zymo Research Quick DNA/RNA™ FFPE Kit, following the manufacturer's instructions. Total RNA was eluted in 50 μL of DNase/RNase-free water. The quantity and purity of the extracted RNA were assessed by measuring the A260/A280 and A260/A230 ratios using a NanoDrop 8000 spectrophotometer (Thermo Fisher Scientific). RNA concentrations were additionally quantified using the Qubit RNA High Sensitivity Kit and a Qubit 4 instrument.

Table 1
Clinical characteristics of PCa patients (good and poor responders). Clinical data was sourced from the oncology centre at National Hospital in Bloemfontein, Free State.

Patient Categories					
Good Responders	**5**	**15**	**16**	**20**	
Clinical stage	IV	IV	IV	IV	
Symptomatic improvement	Yes	Yes	Yes	Yes	
Gleason Score (GS)	7(3 + 4)	7(4 + 3)	8 (4 + 4)	7(4 + 3)	
Grade group (Gg)	2	3	4	3	
Serum PSA Level	n/a	4514	8320 ng/ml	7 μg/l	
Number of cycles of Docetaxel (months)	2–10	2–10	2–10	2–10	
Progressive disease	No	No	No	No	
Age	66	53	55	57	
Excised tissue: Tumour (T)/Normal (N)	T & N	T & N	T & N	T & N	
Poor Responders	**4**	**7**	**13**	**17**	**18**
Clinical stage	IV	IV	IV	IV	IV
Symptomatic improvement	No	No	No	No	No
Gleason Score (GS)	7(4 + 3)	9(4 + 5)	8(4 + 4)	8(4 + 4)	8(5 + 3)
Grade group (Gg)	3	4	n/a	4	4
Serum PSA Level	75 ng/ml	1080	n/a	2874 μg/ml	9287
Number of cycles of Docetaxel (months)	2–10	2–10	2–10	2–10	2–10
Progressive disease	Yes	Yes	Yes	Yes	Yes
Age	56	61	68	57	67
Excised tissue: Tumour (T)/Normal (N)	T&N	T&N	T&N	T&N	T&N

2.3. RNA integrity tapestation analysis

FFPE RNA integrity was evaluated using the 4200 TapeStation RNA ScreenTape and RNA High Sensitivity ScreenTape (Agilent Technologies) capillary electrophoresis systems, following the manufacturer's instructions. The RNA Integrity Number (RIN) and DV200 values were determined using the TapeStation Analysis Software 5.1.

2.4. SPUD quantitative RT-PCR inhibition assay

The SPUD assay was performed as described by (Nolan et al., 2006). In brief, a 100 μM stock solution of the 101 bp SPUD template (Integrated DNA Technologies) was serially diluted ten-fold to a working concentration of 10^{-5} nM (the 10th dilution in the series). Subsequently, 2 μL of the diluted template, 0.25 μM of both forward and reverse SPUD primers (IDT), and 1x PowerUp SYBR Green Master Mix (Thermo Fisher) were combined with 1 μL of FFPE RNA in a total reaction volume of 10 μL in a MicroAmp Optical 384-well reaction plate (Thermo Fisher). A negative inhibition control was prepared by replacing the RNA samples with nuclease-free water. All samples were analysed in triplicate. The plate was sealed with MicroAmp optical adhesive film (Thermo Fisher), and quantitative RT-PCR reactions were carried out using the QuantStudio 12K Flex Real-Time PCR System (Thermo Fisher) under the following cycling conditions: an initial denaturation at 95 °C for 10 min, followed by 40 cycles of 15 s at 95 °C for denaturation, and 1 min at 60 °C for annealing/elongation. Fluorescence data were collected at the end of each annealing/elongation step at 60 °C. This was followed by a melt curve analysis, starting at 95 °C and gradually decreasing from 60 °C to 95 °C in 0.05 °C increments. Data analysis was performed using QuantStudio 12K Flex Software v1.2.4, and the Cq values were calculated using Microsoft Excel.

2.5. Primer design and preparation for quantitative RT-PCR

Quantitative RT-PCR primers for the target gene ABCC1 were designed using the NCBI Primer-BLAST software (http://www.ncbi.nlm.nih.gov/tools/primer-blast/), with the parameters outlined in Table 3 to generate amplicons between 80 and 200 bp. Primers for the housekeeping genes GAPDH, HPRT1, and HSPCB were sourced from the literature and had been previously validated (Table 2). Primer sequences for ABCC10 were obtained from the PrimerBank database (https://pga.mgh.harvard.edu/primerbank/). The quantitative RT-PCR primers were purchased from IDT and resuspended in TE buffer (10 mM Tris, pH 8.0, 1 mM EDTA) to a final concentration of 100 μM, in accordance with the manufacturer's instructions.

2.6. cDNA synthesis

cDNA was synthesized from 100 ng of FFPE total RNA using the Maxima H Minus cDNA Synthesis Master Mix with dsDNase Kit, following the manufacturer's protocol (Thermo Fisher Scientific Pub. No. MAN0016393, Rev.B.0). Additionally, 1 μg of commercial XpressRef Universal Total RNA (QIAGEN) was reverse transcribed and used as a positive control to validate the quantitative RT-PCR assays. NRT (No Reverse Transcriptase) negative control reactions were performed concurrently to assess genomic DNA contamination in the RNA sample. An NTC (No Template Control) reaction was also conducted to check for reagent contamination and the presence of primer dimers.

Table 3
Primer-BLAST primer design selection criteria.

Primer Design Criteria	Selected Parameters
Primer Location	3′- end
PCR product size (bp)	Min = 80 Max = 200
Primer Tm (°C)	Min = 60 Opt = 63 Max = 65
Max. Tm difference [°C] between the primers	1
Primer size (nucleotides)	Min = 18 Opt = 21 Max = 24
Primer GC content (%)	Min = 40 Max = 60
GC clamp	1
Max Poly-X	3
Max GC in primer 3′ end	3
SNP handling	Primer binding site may not contain known SNP
Intron inclusion	Primer separated by at least one intron on the corresponding genomic DNA
Intron length range	Min = 200

2.7. cDNA preamplification

For FFPE cDNA pre-amplification, the TaqMan PreAmp Master Mix (Thermo Fisher) was used according to the manufacturer's instructions. All quantitative RT-PCR primers were pooled by combining 1 μL of each 100 μM primer stock, resulting in a final volume of 200 μL in TE buffer, with each primer reaching a final concentration of 500 nM. The pre-amplification reaction was performed in a 5 μL volume, consisting of 2.5 μL of TaqMan PreAmp Master Mix, 0.5 μL of the pooled primer mix, and 2 μL of cDNA. Amplification was carried out using the following cycling conditions: one cycle at 95 °C for 10 min, followed by 14 cycles of 95 °C for 15 s and 60 °C for 4 min. After the cycling program, the reactions were diluted in TE buffer at a 1:20 ratio. The pre-amplified DNA samples were stored at −20 °C for subsequent quantitative RT-PCR assays.

2.8. Quantitative RT-PCR reaction efficiency

Quantitative RT-PCR efficiency was assessed using standard curves generated from two- and ten-fold dilutions of XpressRef Universal Total cDNA for each target gene. Real-time quantitative RT-PCR amplifications were performed in triplicate, using a total reaction volume of 10

Table 2
Primer nucleotide sequences and product lengths for the target and reference genes amplification by quantitative RT-PCR.

Gene Symbol	Primer name	Primer sequence (5' ———3')	Amplicon size	Reference
ABCC1	3-abcc1Fp1	AGC CCA AAG TGG AAT CCG GAA G	80 bp	This study
	3-abcc1Rp1	AGT CGG CGG CGT AAT TCT TAG C		
ABCC10	ABCC10pp1F	CGGCCTGCTCTATGCTCTG	105 bp	PrimerBank ID 312176402c3
	ABCC10pp1R	CCCCGTGCCTGAAGTGTTA		
GAPDH	3-GAPDHFp	AGT CCC TGC CAC ACT CAG	123 bp	Nolan et al. (2006)
	3-GAPDHRp	TAC TTT ATT GAT GGT ACA TGA CAA GG		
HPRT1	HPRT1F	GAC CAG TCA ACA GGG GAC AT	132 bp	Liu et al. (2015)
	HPRT1R	CCT GAC CAA GGA AAG CAA AG		
HSPCB	HSPCBF	TCT GGG TAT CGG AAA GCA AGC C	80 bp	Jacob et al. (2013)
	HSPCBR	GTG CAC TTC CTC AGG CAT CTT G		

µL, which included 5 µL of 2x PowerUp SYBR Green Master Mix (Thermo Fisher), 0.5 µL of each forward and reverse primer (at a final concentration of 500 nM), 2 µL of nuclease-free water, and 2 µL of cDNA. The reactions were carried out on the QuantStudio 12K Flex PCR System (Applied Biosystems) under the following cycling conditions: 2 min of UDG activation at 50 °C, 2 min of polymerase activation at 95 °C, followed by 40 cycles of 15 s at 95 °C and 1 min at 57 °C, with a subsequent dissociation curve analysis. Standard curves were generated by plotting the CT values against the logarithm of each serial dilution.

2.9. Quantitative RT-PCR assay

Quantitative RT-PCR was performed with a total reaction volume of 10 µL, consisting of 2 µL of diluted pre-amplified cDNA as the template, 5 µL of 2x PowerUp SYBR Green I Master Mix (Thermo Fisher), and 0.5 µL each of forward and reverse primers at a final concentration of 500 nM. No-template control (NTC) reactions were included in all assays as negative controls, and each reaction was conducted in triplicate. The reactions were carried out on the QuantStudio 12K Flex Real-Time PCR System (Applied Biosystems) with the following cycling parameters: 50 °C for 2 min, initial denaturation at 95 °C for 2 min, followed by 40 cycles of 95 °C for 15 s and 57 °C for 1 min. A melt curve analysis was performed for all reactions at the end of the PCR run using default parameters. Amplification data were analysed using Life Technologies QuantStudio 12K Flex Software v1.2.4, applying user-defined thresholds to determine Cq values. Outliers in technical replicates, reactions with no amplification, and reactions displaying multiple Tm peaks during melt curve analysis were excluded from the analysis. The data were then exported into Excel spreadsheets for further analysis.

2.10. Reference gene stability

The stability of the reference genes was assessed using the web-based tool RefFinder (https://blooge.cn/RefFinder/), which employs four established algorithms—GeNorm, BestKeeper, NormFinder, and comparative delta-CT—to simultaneously compare and rank the three candidate reference genes, from the most to the least stable (Xie et al., 2023).

2.11. Statistical analysis

Data are presented as mean ± SD. Experimental data were electronically recorded using Microsoft Excel. The Student's t-test and Mann-Whitney test were employed to assess differences between tumour and normal sections of patient samples in the good vs. poor responder groups. A p-value of <0.05 was considered indicative of a statistically significant difference. All statistical analyses and graphs were generated using GraphPad Prism 10.0.2 (GraphPad Software, Boston, USA).

3. Results

3.1. RNA quantity and quality

Data on RNA quantity (concentration) and quality (A260/A280 and A260/A230 ratios, RIN, DV200) are presented in Table 4. The A260/A280 ratio measures protein contamination, while the A260/A230 ratio reflects the presence of organic contaminants in the sample (Adams, 2020). The precision of these measurements is enhanced by the RNA Integrity Number (RIN), which evaluates the overall quality of the RNA, with a maximum value of 10 representing optimal quality (Adams, 2020). All samples exhibited a DV200 > 30 %, indicating that the RNA was suitable for real-time PCR. An A260/A280 ratio below 1.8 suggests the presence of impurities, which may interfere with downstream enzymatic reactions. For most patients in both the good and poor responder categories, the A260/A280 absorbance ratios were above 1.8. The RNA purity results presented in Table 4 are consistent with those reported by (Kokkat et al., 2013), who found A260/A280 values ranging from 1.95 to 2.18 in RNA extracted from FFPE blocks of various cancers, including malignant lung, thyroid, and salivary gland tissues. Furthermore, these results are in agreement with studies published by (Yi et al., 2020), who reported an RNA purity of 2.0 ± 0.1 at A260/280, and by (Choi et al., 2017), who observed RNA purity values ranging from 1.78 to 2.04. Table 4 also presents the RNA concentrations obtained from patient samples using the Qubit RNA HS Assay Kit. Most samples from both the good and poor responder groups had RNA concentrations exceeding 10ng/µL, with the exceptions of samples 5N (good responder), 17N (poor responder), and 18N (poor responder), which displayed RNA concentrations below 10 ng/µL. An RNA concentration of 10 ng/µL is considered sufficient for downstream applications (Yi et al., 2020).

Table 4
Total RNA quantity and quality in tissue sections categorized as Good responders and Poor responders. (T) Marks tumour section, (N) marks normal section. OOR - out of range, this sample could not be quantified.

Good Responders					
Sample name	**Barcode**	**Qubit RNA concentration (ng/µl)**	**A260/280**	**A260/230**	**DV200 (%)**
HS/16-8879	5T	43,20	1,76	1,37	57.03
HS/16-8879	5N	6,69	1,9	0,23	68.58
HS/19-1158	15T	100,00	2,01	1,31	59.35
HS/19-1158	15N	37,40	1,88	1,13	60.54
HS/21-2103	16T	62,00	1,88	1,41	61.69
HS/21-2103	16N	19,60	1,79	0,22	57.63
HS/18-7520	20T	46,70	2,01	1,48	57.55
HS/18-7520	20N	13,40	1,56	0,48	48.49
Poor Responders					
HS/16-15167	4T	OOR	2,42	0,03	46.87
HS/16-15167	4N	10,40	1,66	0,23	61.17
HS/16-2331	7T	32,10	2,2	0,52	52.67
HS/16-2331	7N	37,20	1,95	0,34	47.78
HS/21-1773	13T	78,00	1,98	0,85	63.70
HS/21-1773	13N	76,00	2,04	1,32	60.67
HS/18-13038	17T	12,80	1,86	0,77	50.45
HS/18-13038	17N	9,84	1,76	0,33	65.54
HS/19-11900	18T	14,10	1,71	0,95	51.40
HS/19-11900	18N	7,80	1,54	0,03	55.49

3.2. RNA integrity

The integrity of RNA samples was assessed using the RNA Tapestation with RNA ScreenTape and High Sensitivity RNA ScreenTape. Table 5 provides the RNA integrity numbers (RIN) of patients categorized as good and poor responders. A RIN scale of 1–10 is used, where 1 represents completely degraded RNA and 10 represents entirely intact RNA. A RIN of 1.4 or higher has been successfully employed in gene expression assays (Kokkat et al., 2013) In the good responder category, the RIN values ranged from a minimum of 2.1 to a maximum of 3.0, with an average RIN of 2.41. For the poor responder category, RIN values

Table 5
RINs of patients in the good and poor responder categories. (T) Marks tumour section, (N) marks normal section. [-] - Sample concentration outside functional range for RIN measurement.

Good Responders		
Sample Name	Barcode	RIN
HS/16-8879	5T	2,20
HS/16-8879	5N	2,00
HS/19-1158	15T	2,60
HS/19-1158	15N	2,40
HS/21-2103	16T	2,10
HS/21-2103	16N	2,10
HS/18-7520	20T	2,90
HS/18-7520	20N	3,00
Poor Responders		
Sample Name	Barcode	RIN
HS/16-15167	4T	[-]
HS/16-15167	4N	2,30
HS/16-2331	7T	2,40
HS/16-2331	7N	2,10
HS/21-1773	13T	2,00
HS/21-1773	13N	1,70
HS/18-13038	17T	3,10
HS/18-13038	17N	3,80
HS/19-11900	18T	3
HS/19-11900	18N	3,1

ranged from 1.7 to 3.8, with an average of 2.61. These findings are consistent with a similar study by (Choi et al., 2017), which reported RIN values ranging from 1.0 to 6.9 and averages of 1.25–3.43, although their study focused on FFPE samples from breast cancer. Maintaining RNA integrity is essential for generating reliable results. Factors such as improper sample handling, prolonged storage, suboptimal storage conditions, or transportation between laboratories can contribute to RNA degradation. Consequently, a rigorous evaluation of RNA integrity is vital before utilizing RNA samples in downstream applications (Vermeulen et al., 2011).

3.3. SPUD inhibition assay

A SPUD assay, a quantitative PCR-based method, was utilized to evaluate the purity of RNA samples by detecting potential PCR enzyme inhibitors (Vermeulen et al., 2011). Specifically, the SPUD quantitative RT-PCR inhibition assay was employed to identify any inhibitors present in the FFPE RNA samples. All RNA samples exhibited Cq (quantification cycle) values within 0.09 cycles of the negative control, indicating the absence of inhibitors that could interfere with the SPUD assay. The Cq value of an amplification reaction refers to the fractional number of cycles required for fluorescence to reach a specific quantification threshold (Ruiz-Villalba et al., 2021). According to (Vermeulen et al., 2011), a Cq value greater than 1 serves as a cut-off to confirm the presence of SPUD assay inhibitors. Table 6 below presents the SPUD assay results for the patient samples categorized as good and poor responders.

3.4. Quantitative RT-PCR assay optimization and validation

The results of the quantitative RT-PCR validation and specificity assay are presented in Fig. 1 (A-F) as standard curves, PCR efficiencies, and melt curves for the ABCC1 and ABCC10 transporter genes. The PCR efficiencies for ABCC1 and ABCC10 were 103.96 % and 117.96 %, respectively. While the ideal PCR efficiency is 100 %, an efficiency range of 90–110 % is considered acceptable according to the MIQE guidelines (Begicevic and Falasca, 2017). The quantitative RT-PCR primers used in this study demonstrated efficiencies within the acceptable range and exhibited high linearity ($R^2 \geq 0.99$), except for ABCC10, which slightly exceeded the acceptable efficiency range (E = 117.96 %). Additionally,

Table 6
Assessment of RT-quantitative RT-PCR inhibition in the FFPE RNA samples. Cq – Quantification cycle.

Good Responders				
Sample name	**Barcode**	**Cq mean**	**ΔCq (Cq Sample – Cq Control)**	**Inhibition indicated**
HS/16-8879	5T	21,85	0,03	No
HS/16-8879	5N	22,2	0,4	No
HS/19-1158	15T	21,8	0,08	No
HS/19-1158	15N	21,71	−0,01	No
HS/21-2103	16T	21,79	0,01	No
HS/21-2103	16N	21,77	−0,03	No
HS/18-7520	20T	21,75	−0,14	No
HS/18-7520	20N	21,89	0,02	No
Poor Responders				
HS/16-15167	4T	21,81	0,07	No
HS/16-15167	4N	21,73	0,09	No
HS/16-2331	7T	21,82	−0,03	No
HS/16-2331	7N	21,85	0,08	No
HS/21-1773	13T	21,72	−0,09	No
HS/21-1773	13N	21,82	−0,01	No
HS/18-13038	17T	21,74	0,03	No
HS/18-13038	17N	21,7	−0,08	No
HS/19-11900	18T	21,87	0,04	No
HS/19-11900	18N	21,83	0,09	No

the melting curves for ABCC1 and ABCC10 indicated no variation between amplicons (PCR products), confirming that the binding was specific to the primers and free of non-specific binding. All quantitative RT-PCR assays produced single amplicons, as evidenced by the single Tm peaks observed on the melt curves, further verifying the absence of primer-dimer formation and the specificity of the reactions.

3.5. Reference gene selection - evaluation of the stability of the reference genes

HSPCB was identified as the most stable of the three reference genes by all RefFinder algorithms, followed by GAPDH (Table 8). Based on these findings, both HSPCB and GAPDH are recommended for normalizing the Cq values of the target genes during relative quantitative data analysis. Normalization is a critical procedure used to account for variations in template quantity. Housekeeping genes, which are typically constitutively expressed, are employed as reference genes to standardize quantitative RT-PCR results and ensure accuracy (Harshitha et al., 2021).

3.6. Quantitative RT-PCR

The expression values (Cq) for each target and reference gene were analysed and are presented by biological group (tumour vs. normal) in Table 8. This table outlines the Cq values for the target genes (ABCC1 and ABCC10) and reference genes (HSPCB, GAPDH, and HPRT). The Cq values of the reference genes were used to normalize those of the target genes, with the stability rankings of the reference genes shown in

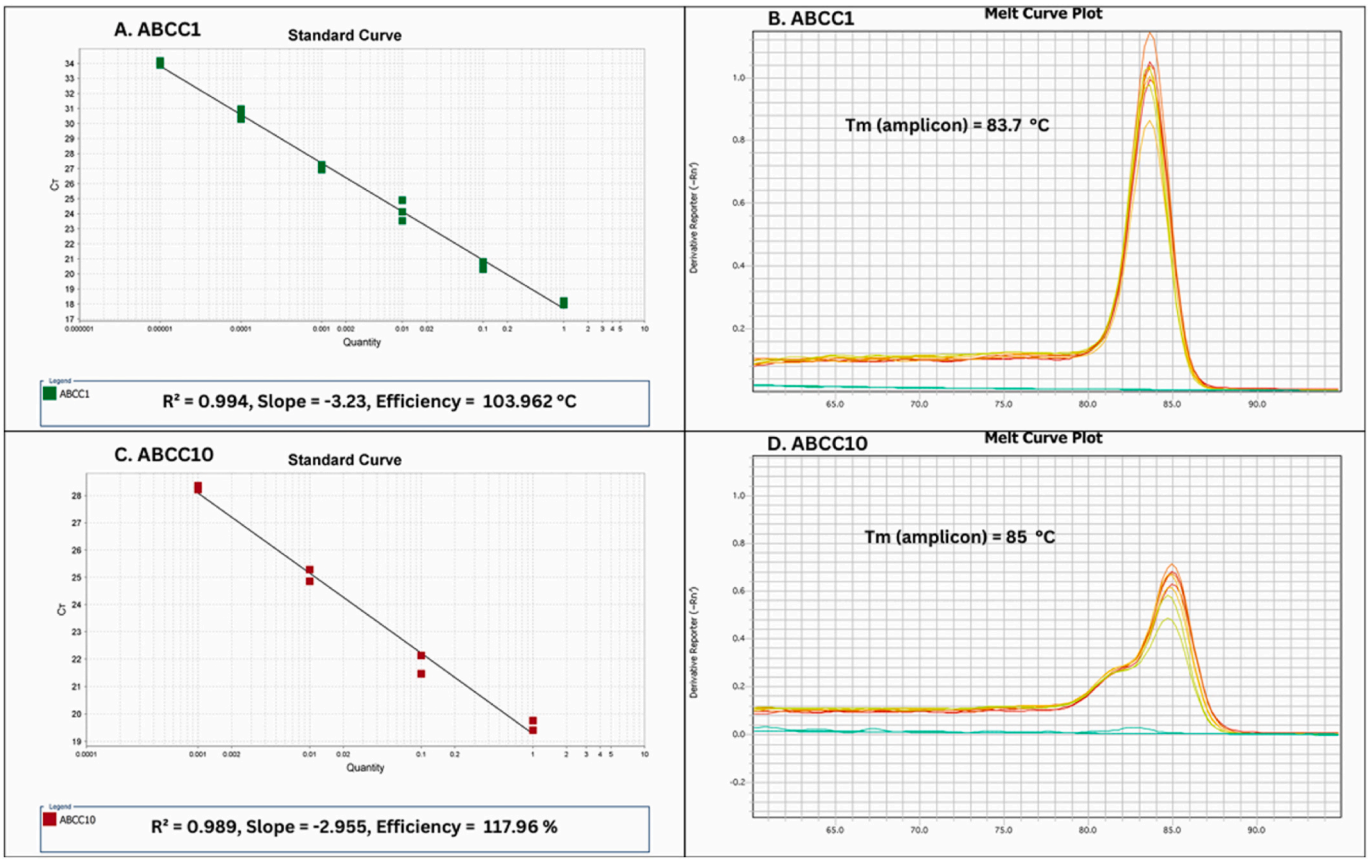

Fig. 1. (A–J): Determination of quantitative RT-PCR efficiencies of target genes (ABCC1 and ABCC10) and reference genes (GAPDH, HPRT, and HSPCB). Standard curves (on the left) using two-fold dilution series of the XpressRef Universal cDNA for ABCC1 (A) and ten-fold dilution series for the rest of the amplicons. CT (Cq) cycles versus log cDNA concentration input were plotted to calculate the slope. The corresponding quantitative RT-PCR efficiencies were calculated using to the equation: E = 10(-1/slope). Melt curve plots (on the right) of quantitative RT-PCR assays show a single Tm peak.

Table 7. In the good responders' category, the Cq values ranged from 18.3 to 21.0 for HSPCB, 16.7 to 20.7 for GAPDH, and 24.8 to 32.6 for HPRT, with HPRT exhibiting the widest range. The target genes ABCC1 and ABCC10 had narrower Cq ranges of 21.6–24.5 and 22.28 to 23.82, respectively, indicating minimal differences between normal and tumour sections.

In the poor responders' category, the Cq values ranged from 17.3 to 27.2 for HSPCB, 15.6 to 29.1 for GAPDH, and 25.4 to 33.8 for HPRT, with HPRT again demonstrating the widest range. ABCC1 and ABCC10 showed broader Cq ranges of 21.0–29.5 and 21.61 to 32.33, respectively, indicating greater variation between normal and tumour sections. Notably, the Cq values for HPRT were undetermined (UND) in samples 5N and 15T in the good responders' category, as well as in samples 7T and 13N in the poor responders' category. In qPCR, an undetermined Cq value indicates that the target gene did not reach the detection limit, implying that HPRT was not expressed in those samples (Pipelers et al., 2017). Overall, the Cq ranges of the reference genes were narrower than those of the target genes in both categories. Furthermore, the Cq ranges for both reference and target genes were lower in the good responders' category compared to the poor responders' category.

3.7. Relative expression levels of target genes

3.7.1. ABCC1 expression in tumour sections: downregulated in good responders and upregulated in poor responders

Fig. 2(A) and (B) illustrates the expression levels of ABCC1 in the normal and tumour sections of prostate cancer (PCa) patients categorized as good or poor responders. In the good responder category, as shown in Fig. 2 (A), ABCC1 expression was significantly downregulated in tumour sections, with an average expression of 0.284, compared to the normal sections, which had an average expression of 12.568. Conversely, in the poor responder category, depicted in Fig. 2 (B), ABCC1 expression was markedly upregulated in tumour sections, with an average expression of 1.083, compared to 0.365 in the normal sections. Additionally, Fig. 3 compares ABCC1 expression in the tumour sections of good and poor responders, showing a 3-fold upregulation in the tumour sections of poor responders relative to good responders. This upregulation of the ABCC1 gene is strongly associated with poor therapeutic outcomes. ABCC1 is a 190 kDa protein encoded by the ABCC1 gene located on chromosome p13.11. It was first identified in H69AR, a doxorubicin-resistant small cell lung cancer cell line, and is closely linked to multidrug resistance (Chen et al., 2021). ABCC1 is predominantly expressed in tissues such as the spleen, colon, breasts, kidneys, testes, lymph nodes, blood-brain barrier, pancreas, brain, and liver (Domenichini et al., 2019). Elevated levels of ABCC1 have been reported in various cancer types, including PCa, non-small cell lung cancer (NSCLC), breast cancer, ovarian cancer, leukemias, melanomas, gastrointestinal carcinomas, and esophageal carcinomas (Sodani et al., 2012).

3.7.2. ABCC10 expression in tumour sections: downregulated in good responders and upregulated in poor responders

The expression of ABCC10 in the tumour and normal sections of patients within the good and poor responder categories is depicted in Fig. 4(A) and (B), while Fig. 5 highlights the expression of ABCC10 specifically in the tumour sections of patients in the good versus poor

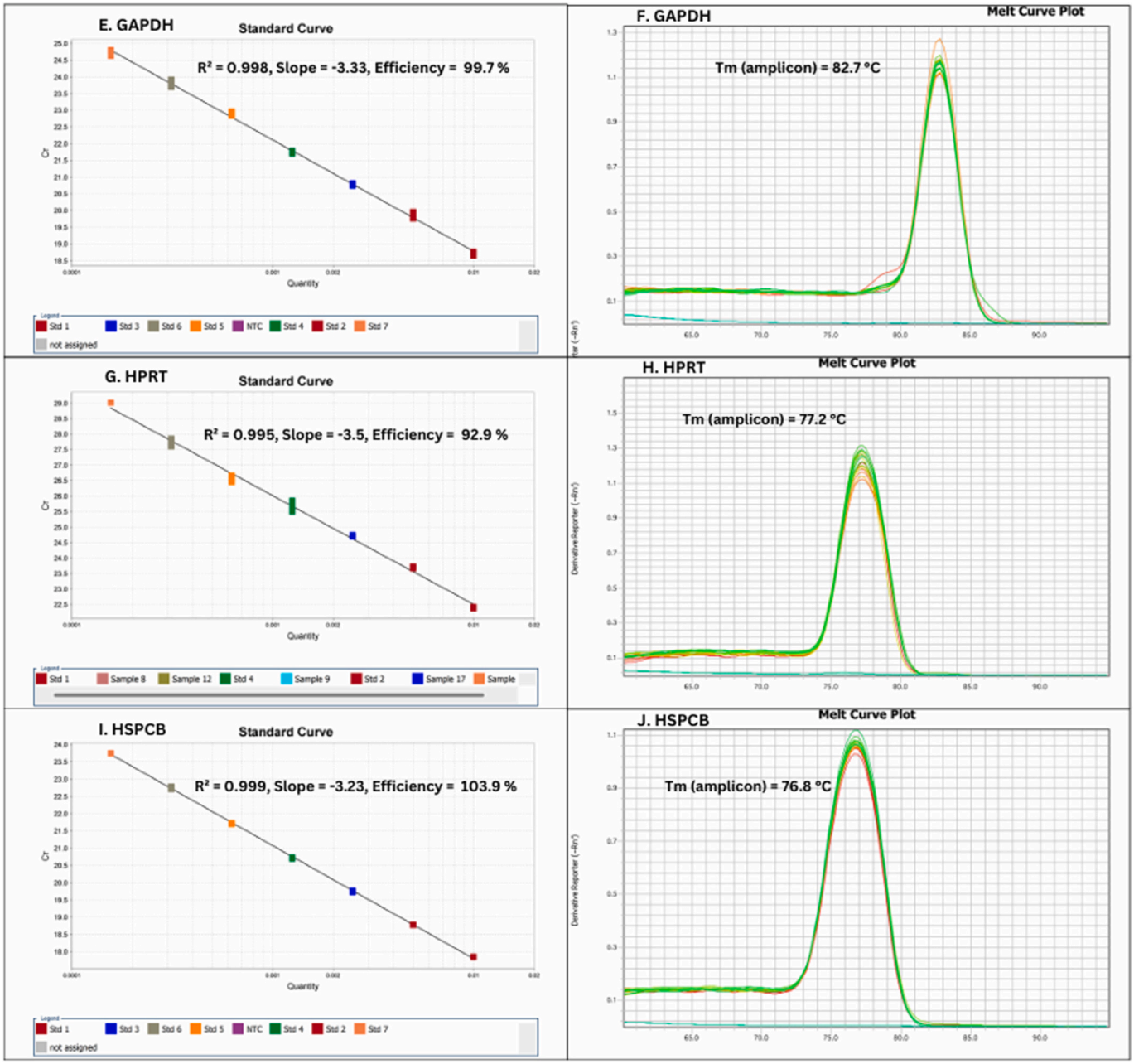

Fig. 1. (*continued*).

Table 7
Ranking and stability values of the three reference genes. The rank order (1–3) for each gene is shown for each algorithm (in parenthesis). The overall rank order of the reference genes is shown.

Reference Gene Stability			
Algorithm	HSPCB	GAPDH	HPRT
ΔCT	1	2	3
BestKeeper	1	2	3
NormFinder	1	2	3
GeNorm	1	1	3
Overall Rank	1	2	3

responder categories. ABCC10 functions as a transporter of lipophilic anions and plays a critical role in detoxification processes (Domenichini et al., 2019). It is also implicated in conferring resistance to various natural product-based chemotherapeutic agents, including a significant resistance to docetaxel (Sodani et al., 2012).

In Fig. 4 (A), **ABCC10** expression was downregulated in the tumour sections of patients in the good responder category, with an average expression level of 0.780, compared to an average of 31.352 in the normal sections. In contrast, Fig. 4 (B) demonstrates that **ABCC10** was significantly upregulated in the tumour sections of patients in the poor responder category, with an average expression level of 3.459, compared to an average of 0.609 in the normal sections. Additionally, Fig. 5 shows a 5-fold upregulation of **ABCC10** in the tumour sections of patients in the poor responder category relative to the tumour sections of those in the good responder category. This finding suggests that the **ABCC10** transporter gene may have actively effluxed docetaxel before it could exert its therapeutic effect. Such activity likely contributed to tumour progression and, ultimately, poor treatment outcomes in patients categorized as poor responders.

Table 8
Mean Cq values (of three replicates) for each target and reference gene using preamplified cDNA samples as templates for quantitative RT-PCR. UND, Cq value undetermined. Positive control sample: XpressRef universal total RNA (QIAGEN) for gene expression.

Good Responders						
Sample Name	**Biological Group**	**Cq^{ABCC1}**	**Cq^{ABCC10}**	**Cq^{GAPDH}**	**Cq^{HPRT}**	**Cq^{HSPCB}**
5T	Tumour	22,0	23,54	17,4	26,3	19,6
5N	Normal	21,6	23,68	17,6	UND	19,8
15T	Tumour	22,3	23,13	19	UND	18,9
15N	Normal	21,8	23,2	18,1	28,2	18,3
16T	Tumour	21,8	22,28	16,9	32,6	18,8
16N	Normal	21,8	22,55	16,7	27,3	18,8
20T	Tumour	23,5	23,39	19,6	31,6	20,1
20N	Normal	24,5	23,82	20,70	24,80	21,0
Poor Responders						
4T	Tumour	29,3	28,25	25,9	26,8	27,2
4N	Normal	23,9	25,13	21,4	33,8	22,4
7T	Tumour	22	24,53	18,5	UND	20
7N	Normal	21,9	23,71	17,8	27,7	19,7
13T	Tumour	21,4	21,61	15,9	29,7	17,4
13N	Normal	21,0	21,7	15,6	UND	17,3
17T	Tumour	23,1	24,31	20,3	29,9	20,9
17N	Normal	23,6	25,78	24,2	27,8	22,8
18T	Tumour	25,2	24,53	22,2	28,4	23,2
18N	Normal	29,5	32,33	29,1	25,4	26,5
CTRL	Control sample	21	21,71	14,1	22,1	14,8

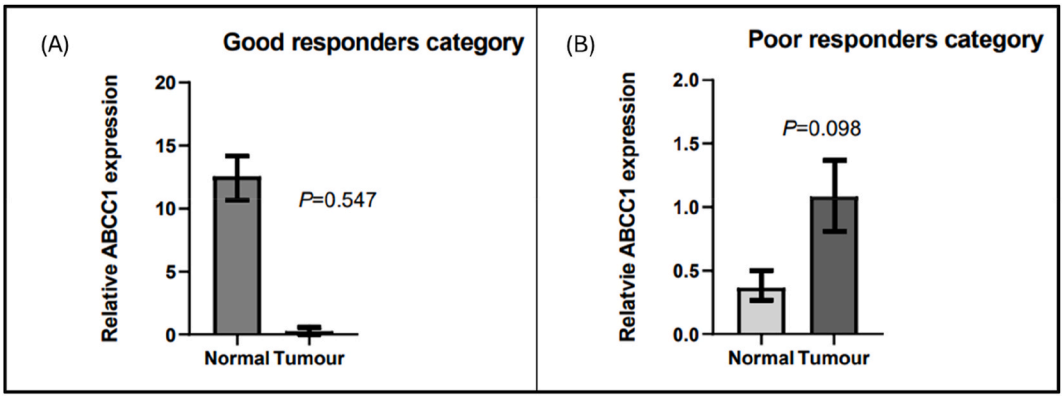

Fig. 2. Expression of ABCC1 in the Prostate tumour and normal tissues. (A), good responder category, $P = 0.547$. (B), poor responder category, $P = 0.098$. Values = mean ± SD; n = 3. Scale determined by GraphPad Prism.

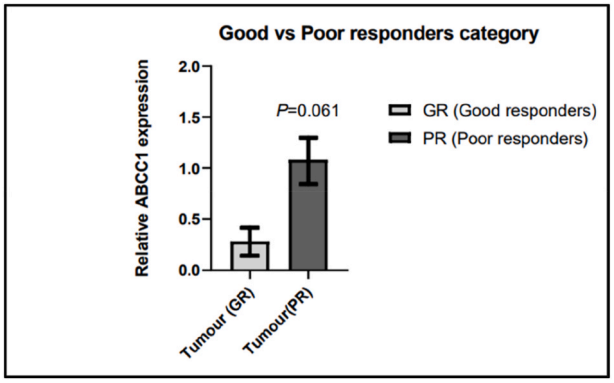

Fig. 3. Expression of ABCC1 in the Prostate tumour and normal tissues of patients in the good vs poor responder categories. Values = mean ± SD; n = 3. $P = 0.061$. Scale determined by GraphPad Prism.

4. Discussion

This study investigated the expression of ABC transporter genes, ABCC1 and ABCC10, as potential predictive biomarkers in PCa patients undergoing docetaxel treatment. The study cohort consisted of patients categorized into good and poor responders based on their clinical response to docetaxel therapy. Table 1 presents the clinical characteristics of both groups, including age, clinical stage, and the number of docetaxel treatment cycles received. Good responders demonstrated sensitivity to docetaxel, exhibiting clinical improvement, whereas poor responders exhibited resistance with no observed therapeutic benefit. The patient cohort ranged in age from 53 to 68 years, consistent with epidemiological evidence associating advanced age with increased PCa risk (Ng, 2021). All patients were diagnosed with metastatic stage IV PCa and underwent 2–10 cycles of docetaxel, which remains the first-line treatment for metastatic PCa (Loblaw et al., 2013).

While age itself does not directly influence chemoresistance, the clinical stage of the tumour significantly affects therapeutic decision-making and response to treatment, potentially contributing to drug resistance. Although docetaxel provides symptomatic relief and extends survival in metastatic prostate cancer, its efficacy is not universal, and resistance mechanisms remain a significant challenge (Wang et al., 2022). The presence of resistance, as observed in the poor responder group, underscores the role of ABC transporters, including ABCC1 and ABCC10, in mediating reduced intracellular drug retention, ultimately affecting therapeutic outcomes (Seo et al., 2020).

RNA was extracted from 18 excised prostate cancer tissue sections, comprising both tumour and normal samples from the study participants. These samples underwent rigorous quality control before being

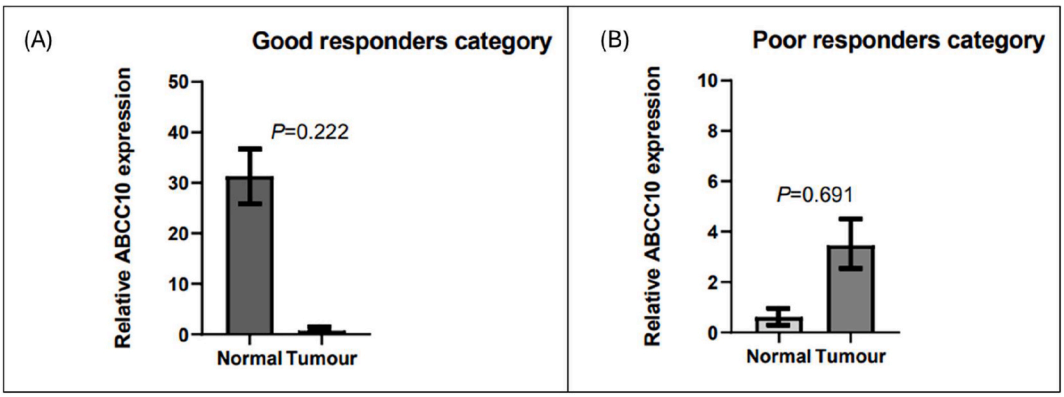

Fig. 4. Expression of ABCC10 in the Prostate tumour and normal tissues. (A), expression of ABCC10 in the good responder category, P = 0.222. (B), expression of ABCC10 in the poor responder category, P = 0.691. Values = mean ± SD; n = 3. Scale determined by GraphPad Prism.

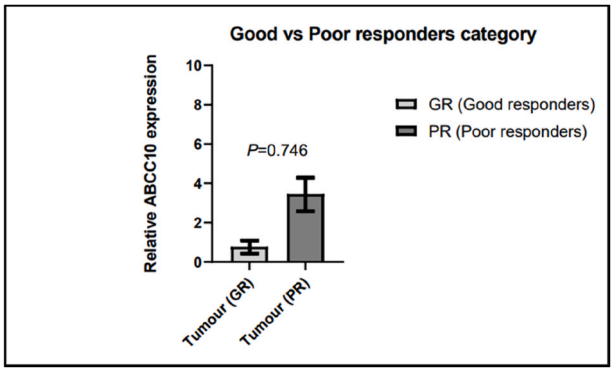

Fig. 5. Expression of ABCC10 in the Prostate tumour and normal tissues of patients in the good vs poor responder categories. Values = mean ± SD; n = 3. *P* = 0.746. Scale determined by GraphPad Prism.

analysed for ABCC1 and ABCC10 expression levels using qRT-PCR. Although multiple anticancer agents have been explored for metastatic castration-resistant prostate cancer (mCRPC), docetaxel was the first to demonstrate a statistically significant survival advantage and remains a cornerstone of treatment (Lima et al., 2021). Notably, even with a modest survival benefit of two to three months, this therapeutic gain is considered clinically meaningful (Parker et al., 2015).

The progression of advanced prostate cancer is ultimately driven by the acquisition of drug resistance, which remains a major obstacle to effective treatment. While the precise molecular mechanisms underlying docetaxel resistance in PCa are not fully elucidated, prior studies have identified various contributing pathways, with increased drug efflux mediated by ABC transporters such as ABCC1 and ABCC10 emerging as a prominent factor (Lima et al., 2021).

Understanding the role of ABC transporters in docetaxel resistance is clinically significant for two key reasons. First, it enables the identification of patients who are unlikely to benefit from chemotherapy, allowing clinicians to explore alternative treatment strategies and avoid unnecessary toxicity. Second, it provides insight into novel therapeutic targets, which may aid in overcoming drug resistance (Mahon et al., 2011). The overarching goal is to stratify patients based on their likelihood of response to chemotherapy and improve treatment outcomes by integrating predictive biomarkers into clinical decision-making (Rodrigues-Ferreira et al., 2021). Thus, uncovering biomarkers and mechanisms of drug resistance is vital for tailoring treatments and improving survival outcomes (Mahon et al., 2011).

ABCC1 is highly expressed in the plasma membranes of various normal tissues, including the intestine, kidney, liver, blood-brain barrier, lung, and peripheral blood mononuclear cells. Its overexpression has been documented in numerous malignancies, including prostate, breast, renal, thyroid, and lung cancers, as well as leukemia and neuroblastoma. Functioning as a lipophilic anion pump, ABCC1 contributes to multidrug resistance by facilitating drug efflux (Xiao et al., 2021). Similarly, ABCC10, another prominent member of the ABC transporter family, is known to mediate resistance to chemotherapeutic agents, including taxanes (docetaxel and paclitaxel), cisplatin, and etoposide, though its precise clinical role remains insufficiently characterized (Zhao et al., 2018; Chen et al., 2011).

The expression levels of ABCC1 and ABCC10 exhibited variation among the FFPE tissue biopsies analysed in this study. Tumour sections from poor responders demonstrated significant overexpression of both transporter genes compared to good responders. Conversely, downregulation of ABCC1 and ABCC10 in good responders correlated with improved treatment outcomes. This downregulation may have facilitated increased intracellular drug accumulation, thereby enhancing docetaxel's therapeutic efficacy and extending its action against tumour cells. These findings suggest that ABCC1 and ABCC10 play critical roles in modulating docetaxel sensitivity and resistance in PCa.

The poor treatment response observed in patients with high ABCC1 and ABCC10 expression may be attributed to the enhanced efflux of docetaxel, reducing its intracellular retention within tumour cells. This diminished drug accumulation likely hindered docetaxel's cytotoxic effect, leading to therapeutic failure and disease progression. The observed association between transporter overexpression and clinical resistance highlights the need for further investigation into targeted strategies to circumvent ABC transporter-mediated drug efflux.

The findings of this study align with those of (Karatas et al., 2016), which reported elevated ABCC1 expression in tumour tissues relative to normal prostate tissue. However, a key distinction lies in the methodologies employed: whereas (Karatas et al., 2016) extracted RNA from radical prostatectomy specimens, the present study utilized FFPE tissue blocks from PCa patients. Moreover (Karatas et al., 2016), focused on recurrent versus non-recurrent PCa and reported no significant difference in ABCC10 expression between tumour and normal samples. In contrast, this study identified increased ABCC10 expression in the tumour sections of poor responders and reduced levels in corresponding normal tissues. Furthermore, the expression levels of ABCC1 in the tumour sections of poor responders (chemo-resistant) in this study align with findings by (Wang et al., 2022), which reported increased ABCC1 levels in PC-3 docetaxel-resistant cells via qRT-PCR. Conversely (Linke et al., 2022), observed very low ABCC10 expression in both docetaxel-resistant and control DU-145 and PC-3 cells, with ABCC1 partially expressed but downregulated in resistant DU-145 and PC-3 cells compared to controls. These findings contrast with the current study, where both ABCC1 and ABCC10 were overexpressed in tumour sections of patients in the poor responders (chemo-resistant) category.

The overexpression of ABC transporters has been linked to increased

drug efflux, resulting in reduced intracellular drug concentrations, diminished treatment efficacy, and the development of a drug-resistant phenotype. Specifically, ABCC10 has been implicated in resistance to docetaxel and other taxanes (Sone et al., 2019). Similarly, ABCC1 has been associated with increased tumour proliferation, inhibition of apoptosis, and enhanced chemoresistance (Domenichini et al., 2019). Elevated ABCC1 expression levels have been reported in clinical PCa cases and correlated with adverse clinical outcomes (Sodani et al., 2012; Chen et al., 2011). The findings of this study further support the role of ABCC1 and ABCC10 in contributing to docetaxel resistance in PCa and underscore the potential utility of these transporters as predictive biomarkers for treatment stratification.

This study provides valuable insights into the role of ABCC1 and ABCC10 in docetaxel resistance; however, several limitations must be acknowledged. The small sample size (n = 9) requires validation in larger cohorts to enhance the generalizability of the findings. Additionally, the study relied on qRT-PCR without protein-level validation, which could further confirm transporter overexpression. While a correlation between ABCC1 and ABCC10 expression and docetaxel resistance was observed, functional studies are necessary to establish causality. Future research should incorporate larger cohorts, functional assays, and bioinformatics analyses to further validate these findings.

5. Conclusion

This study provides compelling evidence that ABC transporters play a critical role in mediating docetaxel resistance in prostate cancer. The significant upregulation of ABCC1 and ABCC10 in the tumour tissues of poor responders underscores their potential as predictive biomarkers for treatment outcomes. These findings highlight the clinical relevance of targeting ABC transporters to enhance the therapeutic efficacy of docetaxel. Integrating transporter inhibitors or employing personalized treatment strategies—such as optimized chemotherapy regimens or tailored dosing adjustments—could help mitigate resistance and improve patient prognosis. By advancing our understanding of docetaxel resistance mechanisms, this study lays the foundation for biomarker-driven therapeutic approaches in prostate cancer management.

CRediT authorship contribution statement

Nandi Ngesi: Conceptualization, Data curation, Formal analysis, Investigation, Methodology, Project administration, Validation, Visualization, Writing – original draft. **Beynon Abrahams:** Formal analysis, Funding acquisition, Project administration, Resources, Supervision, Validation, Writing – review & editing. **Aubrey Shoko:** Data curation, Formal analysis. **Mamello Sekhoacha:** Conceptualization, Funding acquisition, Project administration, Resources, Supervision, Validation, Writing – review & editing.

Funding

This research was supported by the National Research Foundation Thuthuka funding Instrument (Grant No: 129891).

Declaration of competing interest

The authors declare that they have no known competing financial interests or personal relationships that could have appeared to influence the work reported in this paper.

Acknowledgements

We wish to extend our appreciation to Professor A. Scheriff for the invaluable contribution in identifying, categorizing, and providing anonymized patient data crucial for this research study. Additionally, we sincerely acknowledge Dr. L. Muller and his team for their assistance with the histopathological analysis, which enriched the depth of our findings.

Data availability

Data will be made available on request.

References

Adams, G., 2020. A beginner's guide to RT-PCR, qPCR and RT-qPCR. Biochemist 42 (3), 48–53.
Begicevic, R.-R., Falasca, M., 2017. ABC transporters in cancer stem cells: beyond chemoresistance. Int. J. Mol. Sci. 18 (11), 2362.
Cassim, N., et al., 2021. Prostate cancer age-standardised incidence increase between 2006 and 2016 in Gauteng Province, South Africa: a laboratory data-based analysis. S. Afr. Med. J. 111 (1), 26–32.
Chen, Z.S., Tiwari, A.K., 2011. Multidrug resistance proteins (MRPs/ABCCs) in cancer chemotherapy and genetic diseases. FEBS J. 278 (18), 3226–3245.
Chen, X.-Y., et al., 2021. Overexpression of ABCC1 confers drug resistance to betulin. Front. Oncol. 11, 640656.
Chen, D.-Q., et al., 2024. The role of ABCC10/MRP7 in anti-cancer drug resistance and beyond. Drug Resist. Updates, 101062.
Choi, C.-H., 2005. ABC transporters as multidrug resistance mechanisms and the development of chemosensitizers for their reversal. Cancer Cell Int. 5, 1–13.
Choi, Y., et al., 2017. Optimization of RNA extraction from formalin-fixed paraffin-embedded blocks for targeted next-generation sequencing. Journal of Breast Cancer 20 (4), 393–399.
Domenichini, A., Adamska, A., Falasca, M., 2019. ABC transporters as cancer drivers: potential functions in cancer development. Biochim. Biophys. Acta Gen. Subj. 1863 (1), 52–60.
Harshitha, R., Arunraj, D.R., 2021. Real-time quantitative PCR: a tool for absolute and relative quantification. Biochem. Mol. Biol. Educ. 49 (5), 800–812.
Hasan, S., Taha, R., El Omri, H., 2018. Current opinions on chemoresistance: an overview. Bioinformation 14 (2), 80.
Jacob, F., et al., 2013. Careful selection of reference genes is required for reliable performance of RT-qPCR in human normal and cancer cell lines. PLoS One 8 (3), e59180.
Kachalaki, S., et al., 2016. Cancer chemoresistance; biochemical and molecular aspects: a brief overview. Eur. J. Pharmaceut. Sci. 89, 20–30.
Karatas, O.F., et al., 2016. The role of ATP-binding cassette transporter genes in the progression of prostate cancer. Prostate 76 (5), 434–444.
Kokkat, T.J., et al., 2013. Archived formalin-fixed paraffin-embedded (FFPE) blocks: a valuable underexploited resource for extraction of DNA, RNA, and protein. Biopreserv. Biobanking 11 (2), 101–106.
Lima, T.S., et al., 2021. Molecular profiling of docetaxel-resistant prostate cancer cells identifies multiple mechanisms of therapeutic resistance. Cancers 13 (6), 1290.
Linke, D., et al., 2022. Comprehensive evaluation of multiple approaches targeting ABCB1 to resensitize docetaxel-resistant prostate cancer cell lines. Int. J. Mol. Sci. 24 (1), 666.
Liu, L.-L., et al., 2015. Identification of valid reference genes for the normalization of RT-qPCR expression studies in human breast cancer cell lines treated with and without transient transfection. PLoS One 10 (1), e0117058.
Loblaw, D., et al., 2013. Systemic therapy in men with metastatic castration-resistant prostate cancer: a systematic review. Clin. Oncol. 25 (7), 406–430.
Mahon, K.L., et al., 2011. Pathways of chemotherapy resistance in castration-resistant prostate cancer. Endocr. Relat. Cancer 18 (4), R103–R123.
Ng, K.L., 2021. The Etiology of Prostate Cancer. Exon Publications, pp. 17–27.
Nolan, T., Hands, R.E., Bustin, S.A., 2006. Quantification of mRNA using real-time RT-PCR. Nat. Protoc. 1 (3), 1559–1582.
Parker, C., et al., 2015. Cancer of the prostate: ESMO Clinical Practice Guidelines for diagnosis, treatment and follow-up. Ann. Oncol. 26, v69–v77.
Pipelers, P., et al., 2017. A unified censored normal regression model for qPCR differential gene expression analysis. PLoS One 12 (8), e0182832.
Rodrigues-Ferreira, S., et al., 2021. Predicting and overcoming taxane chemoresistance. Trends Mol. Med. 27 (2), 138–151.
Ruiz-Villalba, A., Ruijter, J.M., van den Hoff, M.J., 2021. Use and misuse of Cq in qPCR data analysis and reporting. Life 11 (6), 496.
Sánchez, C., et al., 2009. Expression of multidrug resistance proteins in prostate cancer is related with cell sensitivity to chemotherapeutic drugs. Prostate 69 (13), 1448–1459.
Sekhoacha, M., et al., 2022. Prostate cancer review: genetics, diagnosis, treatment options, and alternative approaches. Molecules 27 (17), 5730.
Seo, H.K., et al., 2020. Docetaxel-resistant prostate cancer cells become sensitive to gemcitabine due to the upregulation of ABCB1. Prostate 80 (6), 453–462.
Sodani, K., et al., 2012. Multidrug resistance associated proteins in multidrug resistance. Chin. J. Cancer 31 (2), 58.
Sone, K., et al., 2019. Genetic variation in the ATP binding cassette transporter ABCC10 is associated with neutropenia for docetaxel in Japanese lung cancer patients cohort. BMC Cancer 19 (1), 1–9.
Varnai, R., et al., 2019. Pharmacogenomic biomarkers in docetaxel treatment of prostate cancer: from discovery to implementation. Genes 10 (8), 599.
Vermeulen, J., et al., 2011. Measurable impact of RNA quality on gene expression results from quantitative PCR. Nucleic Acids Res. 39 (9) e63-e63.

Wang, S., et al., 2022. Inflammatory molecules facilitate the development of docetaxel-resistant prostate cancer cells in vitro and in vivo. Fund. Clin. Pharmacol. 36 (5), 837–849.
Xiao, H., et al., 2021. Clinically-relevant ABC transporter for anti-cancer drug resistance. Front. Pharmacol. 12, 648407.
Xie, F., Wang, J., Zhang, B., 2023. RefFinder: a web-based tool for comprehensively analyzing and identifying reference genes. Funct. Integr. Genom. 23 (2), 125.
Yi, Q.-q., et al., 2020. Effect of preservation time of formalin-fixed paraffin-embedded tissues on extractable DNA and RNA quantity. J. Int. Med. Res. 48 (6), 0300060520931259.
Zhao, H., et al., 2018. ABCC10 plays a significant role in the transport of gefitinib and contributes to acquired resistance to gefitinib in NSCLC. Front. Pharmacol. 9, 1312.